Biotransformations of Bisphenol A in a Mammalian Model: Answers and New Questions Raised by Low-Dose Metabolic Fate Studies in Pregnant CD1 Mice

Daniel Zalko,[1] Ana M. Soto,[2] Laurence Dolo,[1] Céline Dorio,[1] Estelle Rathahao,[1] Laurent Debrauwer,[1] Robert Faure,[3] and Jean-Pierre Cravedi[1]

[1]Institut National de la Recherche Agronomique, Unite Mixte de Recherche 1089 Xénobiotiques, Toulouse, France; [2]Department of Anatomy and Cellular Biology, Tufts Medical School, Boston, Massachusetts, USA; [3]Laboratoire de Valorisation de la Chimie Fine, Université d'Aix-Marseille III, Marseille, France

We investigated the metabolic fate of a low dose (25 µg/kg) of bisphenol A [2,2-bis(4-hydroxyphenyl)propane] (BPA) injected subcutaneously in CD1 pregnant mice using a tritium-labeled molecule. Analytic methods were developed to allow a radio-chromatographic profiling of BPA residues in excreta and tissues, as well as in mothers' reproductive tracts and fetuses, that contained more than 4% of the administered radioactivity. BPA was extensively metabolized by CD1 mice. Identified metabolite structures included the glucuronic acid conjugate of BPA, several double conjugates, and conjugated methoxylated compounds, demonstrating the formation of potentially reactive intermediates. Fetal radioactivity was associated with unchanged BPA, BPA glucuronide, and a disaccharide conjugate. The latter structure, as well as that of a dehydrated glucuronide conjugate of BPA (a major metabolite isolated from the digestive tract), showed that BPA metabolic routes were far more complex than previously thought. The estrogenicity of the metabolites that were identified but not tested for hormonal activity cannot be ruled out; however, in general, conjugated BPA metabolites have significantly lower potency than that of the parent compound. Thus, these data suggest the parental compound is responsible for the estrogenic effects observed in fetuses exposed to BPA during gestation in this mammalian model. *Key words:* **biotransformation, bisphenol A, BPA, endocrine disruptors, environmental estrogen, fetus, gestation, metabolism, mouse, xenoestrogen.** *Environ Health Perspect* **111:309–319 (2003). doi:10.1289/ehp.5603 available via** *http://dx.doi.org/* **[Online 31 October 2002]**

Bisphenol A [2,2-bis(4-hydroxyphenyl) propane] (BPA) is used in industry as a monomer for the synthesis of polycarbonate plastics and epoxy resins. Polycarbonate plastics are employed to manufacture various materials that come in contact with human food, such as plastic bottles, food containers, and storage and microwave plastic ware. Epoxy resins are used as a polymeric binder in protective inner coatings of food and beverage cans (*1,2*). Unreacted BPA monomers are released from these matrices and migrate into food or beverages (*1,3,4*). Similarly, composites and sealants used in dentistry release BPA monomers into saliva (*5*). BPA can also leach from plastic-containing hazardous waste landfills (*6*). Although the biodegradation halflives of BPA in rivers and wastewater treatment plants have been estimated as less than 2 and 4 days, respectively (*7,8*), trace amounts of BPA have been detected in drinking water (*9*). Given these parameters, human exposure to trace amounts of BPA is expected to be relatively low but of daily occurrence.

Adverse effects of BPA on human and animal reproduction are suspected, because it is now well established that BPA is an estrogenic chemical (*10,11*) able to interact with human estrogen receptors (*12*). However, BPA, like most endocrine-disrupting chemicals, is several orders of magnitude less potent than 17β-estradiol. Because of the low expected exposure and the low potency of this compound, it was assumed that the probability of reproductive effects was negligible. However, *in utero* exposure to low doses of BPA (between 2 and 50 µg/kg) induced alterations of the reproductive organs such as increased prostate size (*13,14*) and decreased epididymal weight. Similar results were obtained with low doses of other estrogens, including diethylstilbestrol (DES). Because some attempts to replicate these studies have been unsuccessful (*15,16*), the issue of low-dose effects became controversial (*17*). Several publications since then have confirmed and extended the original observations by the vom Saal group (*18*). For example, Gupta showed increased prostate weight, decreased epididymal weight both *in vivo* and in organ culture, and enhanced anogenital distance (*19*). A possible mechanism through the induction of androgen receptor was postulated (*19,20*). In addition, prenatal exposure in rats altered the histoarchitecture of the prostate (*21*).

Females are also affected by perinatal exposure to BPA. For example, BPA advances the onset of puberty (*22*) and alters mammary gland development in mice (*23*), and it disrupts estrous cyclicity and decreases LH levels after long-term ovariectomy in rats (*24*). These effects occur at doses several orders of magnitude below those needed to evoke a uterotrophic effect (*25*). Because BPA is not the sole source of xenoestrogen exposure in humans, it is likely these chemicals act additively among themselves and with natural estrogens (*26–28*), thus producing effects at very low doses.

The adverse effects of BPA may not be limited to the genital tract and mammary glands. Behavioral disorders were evidenced in Wistar rat offspring when mothers were administered BPA during pregnancy and lactation (*29,30*); both experiments used doses well below the no observed adverse effect level of 50 mg/kg/day. *In vitro*, the mutagenicity of low concentrations of BPA was demonstrated using human (*31*) and Syrian hamster (*32*) embryo cells. In addition, it was demonstrated that BPA could be converted *in vitro* to bisphenol *o*-quinone, a reactive intermediate able to bind irreversibly to DNA (*33*).

Understanding the metabolic routes followed by BPA in mammals is a necessary step for scientists trying to assess the risk associated with the wide use of this chemical. Indeed, both the pharmacologic and the toxicologic properties of BPA may be modified when the parental compound is metabolized. The earliest BPA metabolism study was carried out in 1966 on rats dosed orally with 800 mg/kg BPA (*3*), showing that BPA metabolites were mainly excreted via feces, in which unchanged BPA and its glucuronic acid (GlcA) conjugate (GlcA-BPA) were the major compounds identified. Urine was also an important excretion pathway and apparently contained mainly GlcA-BPA. The same authors have also hypothesized the formation of a hydroxylated metabolite of BPA. Most of these findings have been confirmed by recent studies in mice and rats. Much of the attention has been focused on GlcA-BPA, and it is now accepted that this metabolite is the major residue of BPA both *in vivo* (*34–36*) and *in vitro* (*37–40*), including studies carried out using human liver microsomes (*39*). It has been established that GlcA-BPA

Address correspondence to D. Zalko, INRA, UMR 1089 Xénobiotiques, 180 Chemin de Tournefeuille, BP3, 31931 Toulouse Cédex 9, France. Telephone: 33 5 61 28 50 08. Fax: 33 5 61 28 52 44. E-mail: dzalko@toulouse.inra.fr

We thank R. Gazel, A. Debrusse, E. Perdu-Durand, C. Michaelson, C. Wieloch, and J. Calabro for excellent technical support.

These studies were supported in part by NIEHS grant ES-08314.

Received 12 March 2002; accepted 25 July 2002.

and 3-hydroxy-BPA have estrogenic potencies much lower than that of BPA (*38,39,41*), and that these metabolites are not expected to play a role in the reproductive toxicity of BPA. More is known about the pharmacokinetics of BPA, mainly in rodents (*9,34,42–44*). BPA is quickly absorbed whatever the administration route, but its bioavailability is lower when distributed orally compared with a parenteral administration (*35*). Enterohepatic recirculation of BPA residues has been hypothesized by several authors (*43*). The passage of BPA through the placental barrier and into milk was also demonstrated (*9,36*). However, hardly any data have been published about the nature of BPA residues in maternal tissues and fetuses, and its metabolic fate when low doses are administrated remains to be investigated.

Combining the use of radio–high-performance liquid chromatography (HPLC) and various analytic techniques, we have started an extensive study of BPA metabolism in pregnant CD1 mice. This animal model was chosen because most of the laboratories studying low-dose effects of BPA and other xenoestrogens are using this model (*19,23,45,46*). In addition, rodent placentation at late stages of gestation is histologically close to human placentation, both being of the chorio-allantoidian type with histiotrophic embryo nutrition. To better understand the fate of this xenoestrogen and its possible significance when administered at a low dosage, we administered a subcutaneous dose of 25 μg/kg BPA to CD1 mice at day 17 of gestation and sacrificed them at 0.5, 2, or 24 hr after administration. We then tried to assess a precise residue quantity, as well as metabolic profiles associated with BPA residues in tissues, including fetuses. Additional studies were performed to explore the fate of BPA when administered orally at 25 μg/kg to CD1 mice and to identify metabolites. To achieve mass spectral characterization of BPA residues in the pregnant CD1 mouse, additional animals were dosed by subcutaneous route at 50 mg/kg.

Materials and Methods

Chemicals

^{3}H-labeled BPA [(^{3}H-BPA); 2,2-bis (4-hydroxyphenyl)propane] was purchased from Moravek Biochemicals (Mercury Lane, Brea, CA, USA) with a specific activity of 185 GBq/mmol. It was stored in ethanol at –20°C. In these conditions, only limited tritium exchange occurred (< 3%/6 months). Before the experiments, the solution was evaporated to dryness under a nitrogen stream and resuspended in ethanol. Its purity was greater than 99.9% based on radio-chromatographic analysis. Unlabeled BPA (> 99% pure) was purchased from Sigma Aldrich (L'Isle d'Abeau Chesnes, France).

Other chemicals, solvents (analytic grade), and scintillation cocktails were purchased from the following sources: ammonium acetate, ammonium carbonate, and sodium citrate, Sigma Aldrich; methanol and acetonitrile, Scharlau Chemie S.A. (Barcelona, Spain); ethanol, citric acid, and acetic acid, Merck (Briare-Le-Canal, France).

Apparatus

Radioactivity in urine and all other liquid samples was determined by direct counting on a Packard scintillation analyzer (Model Tricarb 2200CA; Packard Instruments, Meriden, CT) using Packard Ultima Gold as the scintillation cocktail (Packard Instruments, Downer Grove, IL). Radioactivity in mice carcasses, tissues, feces, and extraction pellets was determined by complete combustion using a Packard Oxidizer 306 (Packard Instruments), followed by ^3H_2O quantification on the Packard scintillation analyzer (scintillation cocktail: Packard Monophase S and Packard Permafluor E+, 14:5, v/v). Three replicates were analyzed for each sample.

Samples were analyzed by HPLC on an HP1050 apparatus (Hewlett Packard, Waldbronn, Germany) equipped with a Rheodyne Model 7125 injector (Rheodyne, Cotati, CA) connected for radioactivity detection to a Radiomatic Flo-One/β A500 instrument (Radiomatic, La-Queue-Lez-Yvelines, France) using Flow-Scint II as the scintillation cocktail (Packard Instruments) to establish metabolic profiles, or to an HP 1050 UV detector set at 270 nm and a Gilson Model 201/202 fraction collector (Gilson France, Villiers-Le-Bel, France) for metabolite purification.

Mass spectrometric experiments were performed using a Finnigan LCQ ion trap spectrometer (Thermo Finnigan, Les Ullis, France) equipped with an electrospray ionization (ESI) source. Typical conditions for recording mass spectra were as follows: spray voltage, 4 kV; capillary voltage, –22V; capillary temperature, 200°C. All mass spectra were acquired using automatic gain control conditions and the helium buffer gas was used as collision gas for mass spectrometry $(MS)^n$ studies. Sample solutions [5–10 ng/μL in methanol/water (1:1, v/v)] were infused at a flow rate of 3 μL/min into the ionization source.

^{1}H and two-dimensional nuclear magnetic resonance (2D-NMR) spectra were acquired on a Bruker Avance DMX 500 spectrometer (Bruker, Wissembourg, France) in CD_3OD solution [50 μg sample/100 μL solvent in a 2.5 tube (outer diameter)]. All measurements were obtained using a Bruker cryoprobe TXI at 30°C with trimethylsylane as standard. All samples were stored and processed in single-use glass flasks or clean glassware, except where otherwise indicated.

Animals

Metabolic fate of bisphenol A in pregnant CD1 mice after subcutaneous administration. After a 6-day adaptation period with free access to water and a standard diet (UAR 210; UAR, Villemoisson-Sur-Orge, France) under a 12-hr light/dark cycle, 11 pregnant CD1 mice purchased from Harlan (Gannat, France) were individually housed in stainless steel metabolic cages at day 17 of gestation with free access to water. Animals were weighed and randomly divided into four lots (I, II, III: $n = 3$; IV: $n = 2$). Calculated mean mice weight was not significantly different between lots.

Lots I, II, and III (metabolic balance). Animals were individually injected with 25 μg/kg ^{3}H-BPA dissolved in peanut oil and adjusted with unlabeled BPA to obtain a final specific activity of 572.2 kBq/μg (lots I, II) or 811.3 kBq/μg (lot III). For each animal, the radioactivity remaining in the syringe and needle used for subcutaneous injection was measured to calculate the quantity of BPA really administered. After 0.5, 2, and 24 hr, respectively, mice from lots I, II, and III were anesthetized with ether and exsanguinated. Blood, liver, peritoneal fat, gall bladder, uterus, and ovaries were collected, as well as the digestive tract, including its content (from duodenum to rectum), and the remaining carcass. Uteri were individually processed to separate fetuses, placenta, amniotic fluid, and the uterus itself. For lot III (24-hr experiment) urine and feces were also collected and metabolic cages were washed with 100 mL ethanol from which aliquots were taken for residual radioactivity determination. All samples were stored at –20°C if not used immediately.

Lot IV (metabolite production for structural characterization). Animals were individually injected with 50 mg/kg of a ^{3}H-BPA solution adjusted with unlabeled BPA to 301.6 Bq/μg and dissolved in peanut oil. Mice were sacrificed as described above 24 hr after BPA dosage. Similar tissue samples were collected, as well as urine and feces.

Bisphenol A metabolism in CD1 mice after oral administration. Three adult nonpregnant female CD1 mice (lot V) were obtained from Harlan, handled in the same conditions as indicated above, and force-fed a single oral dose of 25 μg/kg of a ^{3}H-BPA solution adjusted with unlabeled BPA to 572.2 kBq/μg dissolved in peanut oil. Urine and feces were collected over a 24-hr period, after which animals were sacrificed as described above. Blood, liver, ovaries, uterus, and carcasses were collected for radioactivity quantification. Radioactivity remaining in the material used for injection

was determined to allow actual BPA dosage calculation.

Analytic Procedure

Metabolite profiling. HPLC coupled to on-line radioactivity detection was used for metabolite profiling. The HPLC system consisted of a Zorbax C18 column (250 × 4.6 mm, 5 µm) (Interchim, Montluçon, France) coupled to a Kromasil C18 guard precolumn (18 × 4.6 mm, 5 µm) (Interchim). Mobile phases consisted of ammonium acetate buffer (20 mM, pH 3.5) and acetonitrile 95:5 v/v in A and 10:90 v/v in B, respectively. Flow rate was 1 mL/min at 35°C. A three-step gradient was used as follows: 0–4 min 100% A; 4–6 min linear gradient from 100% A to A:B 85:15 v/v; 6–16 min A:B 85:15 v/v; 16–18 min linear gradient from 15% B to 25% B; 18–28 min A:B 75:25 v/v; 28–30 min linear gradient leading to 100% B; 30–40 min 100% B.

Sample processing. Urine samples were mixed with methanol (1:2, v/v), stirred and centrifuged for 10 min at 6,000 × *g* and 4°C. The pellet was discarded. The supernatant was concentrated under a nitrogen stream before radio-HPLC analysis.

Liver, fetuses, and placenta. For each mouse, liver, pooled placenta, and three fetuses were separately homogenized and the radioactivity present in these samples was determined after combustion. The remaining samples, including the rest of fetuses (pools of three to five, depending on litter size) were processed following an identical procedure: Approximately 5 g of tissue was homogenized with 5 mL/g acetonitrile/methanol/ammonium acetate buffer 40 mM, pH 3.2 (6:3:1, v/v/v), using a Polytron homogenizer (Kinematica, Lucerne, Switzerland), then centrifuged at 8,000 × *g* and 4°C for 10 min. The radioactivity extracted was determined, the supernatant was stored at –20°C, and the pellet was subjected to five additional extractions: twice with the same mixture, then three times using 5 mL/g acetonitrile/methanol/ammonium carbonate buffer 40 mM, pH 8 (6:3:1, v/v/v). Residual radioactivity remaining in the last centrifugation pellet (nonextractable radioactivity) was determined after combustion in an oxidizer. The first two acidic extracts were pooled, delipidated using acetonitrile-saturated isooctane, concentrated under vacuum, and filtered through 45-µm nylon Acrodisc filtering units (Gelman, Ann Arbor, MI, USA) before radio-HPLC analysis.

Feces and digestive tracts (including their contents) were extracted successively six times using the procedure described above, except ethanol (5 mL/g) was used instead of the acidic and basic solvent mixtures. After radioactivity determination, ethanol was added to bile samples (9:1 v/v), that were stirred, centrifuged (10 min, 5,000 × *g*, 4°C), concentrated, and analyzed by radio-HPLC.

Plasma and amniotic fluid. Blood was collected in heparinized tubes and immediately centrifuged at 1,500 × *g* (10 min, 4°C). Radioactivity in red blood cell pellets was determined by combustion in an oxidizer. Radioactivity in plasmas and amniotic fluids was determined by direct counting of aliquots. The remaining material was then extracted and analyzed using the same method as described for bile.

Volatile radioactivity quantification. After extraction, aliquots (typically 20, 40, and 80 µL) were taken for radioactivity determination. Identical aliquots were evaporated to dryness and rediluted in 100 µL ethanol before radioactivity determination. For each sample tested (placenta, amniotic fluid, plasma, and fetuses), this procedure was carried out in triplicate, thus allowing the calculation of the mean percentage of volatile radioactivity.

Metabolite isolation. BPA metabolites were isolated from urine, digestive tract, liver, feces, and fetus samples from lot IV mice. Using the extraction procedure described above, samples were concentrated under a nitrogen stream, rediluted in 10 mL ammonium acetate buffer 50 mM adjusted to pH 3.2, and extracted using an Oasis HLB 0.5 g LP cartridge (Waters, Milford, MA, USA) previously washed with methanol (10 mL) and equilibrated with the buffer (10 mL). Elution was performed successively with 10 mL of the ammonium acetate buffer and then three times with methanol (10 mL). Methanol fractions containing radioactivity (usually only the first one) were concentrated under a nitrogen stream before HPLC separation using the same apparatus as described for the analytic system, but with mobile phases consisting of an acetic acid solution (pH 2.8) and acetonitrile (95:5 and 10:90 v/v in A and B, respectively). Flow rate was 1 mL/min at 35°C. Gradient was as follows: 0–4 min 100% A; 4–39 min linear gradient from 100% A to 100% B; 39–44 min 100% B.

Enzymatic tests. With the methods described above, 600 Bq metabolite F was isolated from fetus extracts (lots I–III). The metabolite was diluted in sodium citrate buffer 0.1 M and its purity was verified by radiochromatography. Assay 1: 10 µL (0.1 unit) *Aspergillus niger N*-acetyl glucosaminidase (Sigma) was added to 150 Bq metabolite F in 300 µL buffer adjusted to pH 4. Assay 2: 10 µL (0.1 unit) chicken liver *N*-acetyl galactosaminidase (Sigma) was added to 150 Bq metabolite F in 300 µL buffer adjusted to pH 3.65. Both incubations were carried out at 37°C for 2 hr. Radio-chromatographic analyses of the incubation media were achieved by spiking separately approximately 50 Bq of the incubates, fortified or not with 50 Bq of the original metabolite. Controls were carried out using similar conditions with no enzyme.

Metabolite identification. For each sample, a 10 ng/µL solution in CH_3OH/H_2O (1:1 v/v) was introduced into the ion source at a flow rate of 3 µL/min. All isolated metabolites were analyzed by MS using negative ESI mode. When necessary, additional analyses were performed using negative ionization mode. MS^n experiments were carried out on the metabolite's quasi-molecular ions, allowing the determination of their structure.

For some metabolites, hydrogen/deuterium (H/D) exchange experiments were performed using CH_3OD/D_2O as the solvent to provide further structural information. Under such conditions, all mobile hydrogen atoms were exchanged with deuterium atoms, resulting in a shift in the *m/z* ratio of the studied ion.

Statistical analysis. Comparison between values was achieved using the Student *t*-test.

Results

BPA Distribution and Residual Levels

The radioactivity remaining in the material used to dose the animals was measured. For mice given a 25 µg/kg nominal dosage, corrected values were 20.9 ± 1.4 µg/kg (lot I), 21.3 ± 1.3 µg/kg (lot II), 22.1 ± 1.4 µg/kg (lot III), and 22.4 ± 1.3 µg/kg (lot V), with no significant difference between groups; mice given 50 mg/kg (lot IV) received an actual dosage of 46.1 ± 2.1 mg/kg BPA.

Twenty-four-hour metabolic balance in pregnant mice dosed subcutaneously with 25 µg/kg BPA (lot III). Residual levels of radioactivity measured in excreta and tissues are summarized in Table 1, with the corresponding concentrations expressed in nanograms per gram ± SD of BPA equivalent. Total recovery for this experiment was 85.7 ± 6.4% of the administered radioactivity. Urine contained less than 6% of the administered radioactivity. The digestive tract (including its contents) contained most of the administered dose (45%); feces contained 21%. Gall bladders contained less than 2% of the administered radioactivity, though for all three mice they were filled with bile. The highest residual levels were found in liver (12 ng/g); it contained about 2.5% of the administered radioactivity. Residual levels calculated for whole blood corresponded to 2.2 ± 0.3 ng/mL, about 85% of these residues being associated with the plasma fraction. In the reproductive tract, residual levels ranged from 2.2 to 4.8 ng/g, respectively, for ovaries and amniotic fluids, whereas fetuses (3.7 ng/g) accounted for a total of 4% of the administered radioactivity, regardless of litter size (9, 13, and 16 fetuses for the three mice).

Comparative study at 0.5, 2, and 24 hr in pregnant mice dosed subcutaneously with 25 µg/kg BPA (lots I, II, III). Radioactivity levels recovered from maternal plasma and liver, placenta, amniotic fluid, and fetuses are summarized in Figure 1, as well as the proportion of the nonextractable, extractable volatile, and extractable nonvolatile (later analyzed by radio-HPLC) radioactivity fractions, respectively. Residual levels are also given for uterus and ovaries, but no extraction was carried out on these low-weight samples.

With the exception of plasma, the highest levels of radioactivity were detected 30 min after BPA administration (lot I). For these mice, the highest concentrations of residues were found in liver, uterus, and placenta (20–40 ng/g), whereas in ovaries, amniotic fluid, and fetuses, levels were in the 10 ng/g range. Because of the large SDs observed in lot I, differences among the three time points were not statistically significant, except for liver ($p < 0.01$) and ovaries ($p < 0.05$). As shown in Figure 1, the amount of nonextractable residues was low at 2 or 24 hr after BPA dosage and was slightly higher at 0.5 hr. The main difference between the 2- and 24-hr points was a higher proportion of volatile radioactivity for the latter lot, representing more than two-thirds of the residues extracted from amniotic fluid, fetuses, and maternal plasma after 24 hr. In liver, relatively high levels of radioactivity were found in extraction pellets, and the proportion of volatile radioactivity remained low even at 24 hr.

Residual levels in pregnant CD1 mice dosed subcutaneously with 50 mg/kg BPA (lot IV). Two animals were used to produce enough material for BPA metabolite isolation and to check a possible change in BPA metabolic routes. Thus, no attempt has been made to compare this lot with the other ones. The mean BPA residual levels measured in liver, ovaries, uterus, amniotic fluid, and fetuses were 14, 1.7, 9.4, 6.4, and 4.3 µg/g, respectively. Radioactivity distribution was comparable to that observed in mice dosed with 25 µg/kg BPA.

Residual levels in CD1 mice dosed orally with 25 µg/kg BPA (lot V). For this lot, residual radioactivity levels measured in blood, ovaries, and uterus (27 ± 9, 21 ± 5, and 160 ± 70 pg/g, respectively) were significantly lower than those obtained for lot III mice ($p < 0.0001$), whereas for liver (6.3 ± 2.4 ppb), the difference was not statistically significant. In contrast, more residues were detected in mouse carcasses after oral dosage (8.0 ± 0.6 ng/g, $p < 0.001$). When submitted to radio-HPLC analysis, urinary and fecal extracts revealed no qualitative difference when compared with lot III mice samples (data not shown).

Table 1. Twenty-four-hour metabolic balance of BPA in pregnant CD1 mice dosed subcutaneously with 25 µg/kg BPA at day 17 of gestation (mean of three animals ± SD).

	Percent of administered radioactivity	ng/g or ng/mL (^{3}H-BPA equivalents)
Blood	0.17 ± 0.06	2.20 ± 0.29
Ovaries	0.01 ± 0.00	2.25 ± 0.26
Uterus	0.40 ± 0.01	3.45 ± 0.13
Placenta	0.55 ± 0.02	3.14 ± 0.34
Amniotic fluid	0.34 ± 0.17	4.85 ± 0.47
Fetus ($n = 3$)	0.33 ± 0.06	3.70 ± 0.38
Fetus (litter[a])	4.13 ± 0.46	
Liver	2.48 ± 0.83	11.95 ± 4.12
Bile	1.87 ± 0.35	1.66 ± 0.32
Digestive tract[b]	45.30 ± 0.38	
Feces	21.23 ± 6.70	
Urine	5.72 ± 1.33	8.16 ± 1.82
Fat	0.01 ± 0.01	0.75 ± 0.22
Carcass	2.75 ± 1.17	1.37 ± 0.58
Cages	0.72 ± 0.34	
Total	85.68 ± 6.42	

[a]Total radioactivity recovered for the whole litter. [b]Total radioactivity recovered from duodenum to rectum, including the digestive tract content.

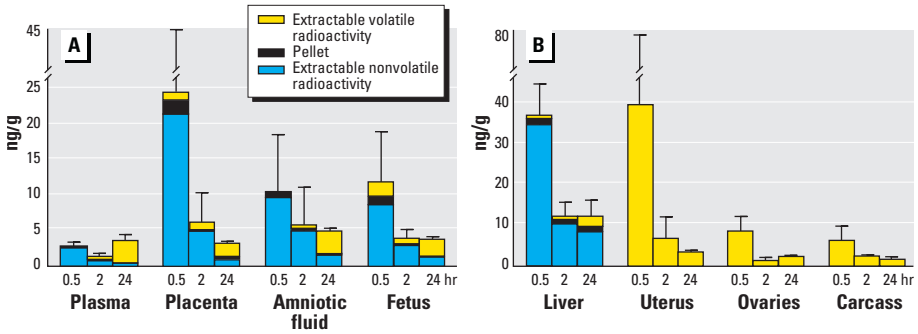

Figure 1. Residual levels of radioactivity measured 0.5, 2, and 24 hr after a subcutaneous injection of 25 µg/kg ^{3}H-BPA to CD1 mice at day 17 of gestation, in (*A*) plasma, placenta, amniotic fluid, and fetus and (*B*) liver, uterus, ovaries, and carcass. Results (mean ± SD, $n = 3$) are expressed in nanograms per gram BPA equivalent.

Qualitative Study of BPA Excretion

The structures of the main BPA metabolites identified in this work are summarized in Table 2, together with their corresponding codes and mass spectral characteristics.

Urinary excretion. The HPLC conditions developed for this study allowed the separation of 10 different radioactive peaks from urine samples. After analysis of all urine samples, no major difference was observed between lots I, II, and III mice (25 µg/kg, subcutaneous dosage), lot IV mice (50 mg/kg), and lot V mice (oral dosage). A representative analysis is shown in Figure 2. Unchanged BPA [retention time (R_t), 33.5 min] was detected in very low quantities in urine, whereas two major metabolites (GlcA-BPA-OH and GlcA-BPA) accounted for more than two-thirds of the radioactivity.

Fecal excretion. Results obtained after the analysis of feces, bile, and digestive tracts are summarized in Table 3 for lot III mice. Fecal radioactivity was mostly associated with unchanged BPA (> 95%), whereas biliary extracts consisted of more than 90% GlcA-BPA. Surprisingly, digestive tract extracts were found to contain, in addition to these two compounds, a third major metabolite of intermediary polarity, later identified as GlcA DH-BPA. A representative radio-chromatogram for pregnant CD1 mice is presented in Figure 3, showing the presence of additional metabolites exhibiting similar R_ts to compounds already detected in urine. Again, no major qualitative differences were observed for lots IV and V.

Metabolite identification. All structural characterizations have been achieved on material isolated from lot IV mice, using negative ionization ESI/MS^n. Additional details and mass spectral data are summarized in Table 2. The structure of unchanged BPA (R_t, 33.5 min) was confirmed for all analyzed tissues where it was detected.

GlcA-BPA, with an R_t of 25 min, was the major metabolite in urine and digestive tract extracts. It was directly characterized from both matrices as well as from liver extracts. $[M–H]^-$ ion was detected at *m/z* 403. In MS^2 experiments, fragmentation of this quasi-molecular ion led to the pair of complementary fragment ions at *m/z* 277 (corresponding to deprotonated BPA) and *m/z* 175, characteristic

of a glucuronide moiety. The loss of water was also observed (*m/z* 385), probably originating from the glucuronide moiety, because further dissociation of the *m/z* 385 ion in a subsequent MS^3 experiment led to the formation of an *m/z* 227 ion (deprotonated BPA). Thus, this metabolite was identified as the GlcA conjugate of BPA.

GlcA DH-BPA represented about 30% of the radioactivity detected in digestive tracts (lot III), thus accounting for more than 15% of the BPA residues formed *in vivo*. It was isolated from this matrix. $[M–H]^-$ quasi-molecular ion was detected at *m/z* 385, and the MS^2 spectrum of this ion was identical to that of the *m/z* 385 fragment ion produced by water loss from the *m/z* 403 deprotonated ion of GlcA-BPA. These data indicated that GlcA DH-BPA may be a dehydrated form of the GlcA conjugate of BPA.

Additional support for this hypothesis was provided by H/D exchange experiments using CH_3OD/D_2O as the solvent for ESI experiments. In these conditions, the quasi-molecular ion of GlcA-BPA was shifted from *m/z* 403 to *m/z* 407, consistent with the presence of five exchangeable hydrogen atoms in GlcA-BPA, whereas the quasi-molecular ion of GlcA DH-BPA was shifted from *m/z* 385 to *m/z* 388, indicating the presence of four exchangeable

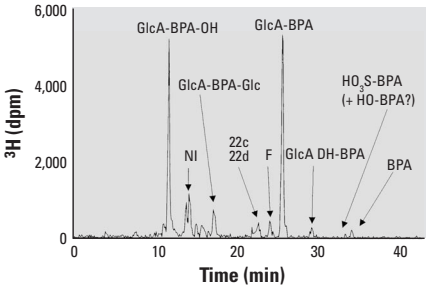

Figure 2. Typical radio-chromatographic profile for 0- to 24-hr urine collected from mice dosed subcutaneously with 25 µg/kg ^{3}H-BPA at day 17 of gestation. Abbreviations: NI, unidentified metabolite; F, R_t corresponding to metabolite F; all other structures are detailed in Table 2.

Table 2. R_t, code, structure, and mass spectral data for most of the BPA metabolites identified in this study.

R_t (min)	Metabolite code (identified from)	Metabolite structure	Quasi-molecular ion $[M–H]^-$ (*m/z*)	Observed fragment ions in ESI-MS^n (*m/z*)
11.5	GlcA-BPA-OH (urine)	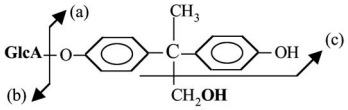	419	(a) 243 (MS^2 419) (b) 175 (MS^2 419) (c) 213 (MS^3 419, MS2 243)
17.5	GlcA-BPA-Glc (urine)	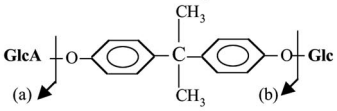	565	(a) 175 (MS^2 565) (b) 403 (MS^2 565) (a) 175 (MS^3 565-403)
22a	HO_3S-BPA-GlcA DH | OH (digestive tract)	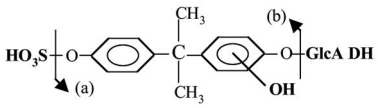	481	(a) 401 (MS^2 481) (b) 243 (MS^3 481-401)
22b	HO_3S-BPA-GlcA DH | OCH_3 (digestive tract)	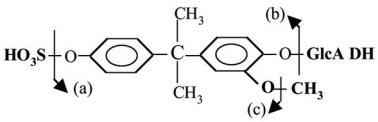	495	(a) 415 (MS^2 495) (b) 257 (MS^3 495-415) (c) 242 (MS^4 495-415-257)
22c	HO_3S-BPA-Glc | OCH_3 (liver, urine)	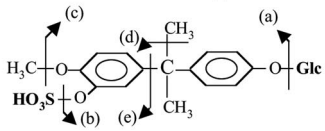	499	(a) 337 (MS^2 499) (b) 257 (MS^3 499-337) (c) 242 (MS^4 499-337-257) (d) 227 (MS^5 499-337-257-242) (e) 109 (MS^6 499-337-257-242-227)
22d	OH | HO_3S-BPA-Glc | OCH_3 (liver, urine)	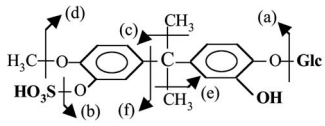	515	(a) 353 (MS^2 515) (b) 273 (MS^3 515-353) (c) 258 (MS^4 515-353-273) (d) 243 (MS^5 515-353-273-258) (e) 228 (MS^6 515-353-273-258-243) (f) 109 (MS^6 515-353-273-258-243)
25	GlcA-BPA (urine, liver, digestive tract)	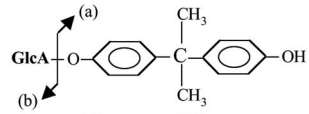	403	(a) 227 (MS^2 403) (b) 175 (MS^2 403)
29	GlcA DH-BPA (digestive tract)	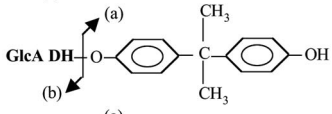	385	(a) 227 (MS^2 385) (b) 157 (MS^2 385)
31.5	HO_3S-BPA (feces, urine)	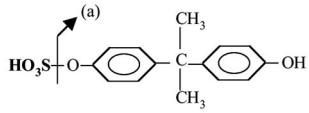	307	(a) 227 (MS^2 307)
32.5	HO-BPA (feces)	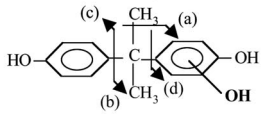	243	(a) 228 (MS^2 243) (b) 149 (MS^2 243) (c) 93 (MS^2 243) (d) 109 MS^2 243)

GlcA DH, dehydrated glucuronide. Metabolites have been isolated from urine, liver, or the digestive tract, as indicated. Because the exact position of conjugation and/or hydroxylations cannot be unambiguously determined by ESI-MS analysis, a different configuration cannot be ruled out for metabolites 22a–22d.

hydrogen atoms in this species (Figure 4). For the latter compound, the MS^2 spectrum of the quasi-molecular $[M_{d4}–D]^-$ ion at *m/z* 388 displayed characteristic fragment ions at *m/z* 344 (CO_2 elimination from the glucuronide moiety), and a pair of complementary fragment ions at *m/z* 228 and *m/z* 158, corresponding to the BPA and the glucuronide moieties, respectively. The *m/z* 158 (instead of *m/z* 157 under nonlabeling conditions) product ion evidenced the occurrence of only one exchangeable hydrogen atom on this fragment ion. Given this information, only one possible position of the double bond in the GlcA moiety allows the formation of a monodeuterated fragment ion at *m/z* 158, according to the decomposition scheme proposed in Figure 4.

To confirm this hypothesis, this metabolite was investigated using ^1H and 2D-NMR, including gradient selection (gs)-correlation spectroscopy, gs-heteronuclear multiple quantum coherence (HMQC), and gs-heteronuclear multiple bonding coherence (HMBC). The 1H NMR spectrum recorded in CD_3OD displayed characteristic signals (Table 4). Beside aromatic signals of BPA (two AB spin systems), of particular importance is the observation of resonances in the sugar region: a triplet for H2′, two doublets for H1′ and H4′, and a double doublet for H3′. Then the structure of GlcA DH-BPA was unambiguously established using 2D-NMR techniques. Moreover, ^{13}C chemical shifts were determined from the F1 projection of HMQC and HMBC diagrams, because the weak amount of metabolite (50 µg) precluded the direct measurement of a carbon spectrum. These results were in agreement with the structure proposed by MS, double-bond resonances being observed for the metabolite. It is worth noting that the signal of carboxylic acid C6′ carbon was not observed, as is frequently the case for glucuronides. Furthermore, long-range correlations in the HMBC spectrum allowed us to rule out any other position for the double bond on the dehydrated form of GlcA.

Thus, the results obtained support the structural characterization of a dehydrated glucuronide conjugate of BPA.

GlcA-BPA-OH, the second major urinary metabolite (R_t, 11.5 min) was isolated from urine. This metabolite exhibited an $[M–H]^-$ ion at *m/z* 419. The fragmentation of this ion (MS^2) led to the formation of the *m/z* 175 (GlcA moiety) and *m/z* 243 fragment ions, the latter likely corresponding to hydroxylated BPA. To get more structural information, the *m/z* 243 fragment ion was submitted to collisional excitation in a subsequent MS^3 experiment. The corresponding mass spectrum displayed characteristic fragment ions at *m/z* 225 (loss of H_2O) and *m/z* 213 (loss of CH_2O), allowing us to locate the hydroxylation site on one of the two methyl groups of BPA.

GlcA-BPA-glucose (Glc), with an R_t of 17.5 min, was isolated from urine. The $[M–H]^-$ quasi-molecular ion was detected at *m/z* 565. The MS^2 spectrum of this *m/z* 565 ion showed fragment ions due to the apparent loss of Glc (*m/z* 403) as well as a GlcA moiety (*m/z* 175). Moreover, MS^3 spectrum of the *m/z* 403 ion was identical to that of the *m/z* 403 $[M–H]^-$ molecular ion of GlcA-BPA. Thus, this metabolite should be considered a GlcA/Glc double conjugate of BPA, as indicated in Table 2.

At least two polar metabolites were detected in urine samples, between the R_t of GlcA-BPA-OH and GlcA-BPA-Glc. These compounds have not been identified. Metabolite F (R_t, 24 min) was detected in low amounts in urine and digestive tract extracts. Its structural characterization was achieved only from liver and fetuses and is detailed elsewhere.

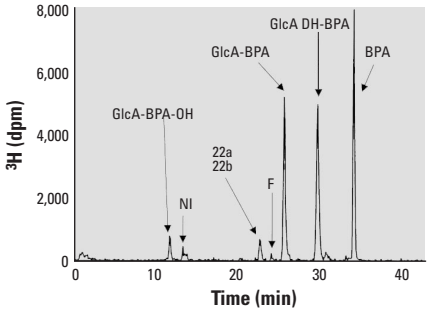

Figure 3. Typical radio-chromatographic profile for 0- to 24-hr feces collected from mice dosed subcutaneously with 25 µg/kg ^3H-BPA at day 17 of gestation. Abbreviations: NI, unidentified metabolite; F, R_t corresponding to metabolite F; all other structures are detailed in Table 2.

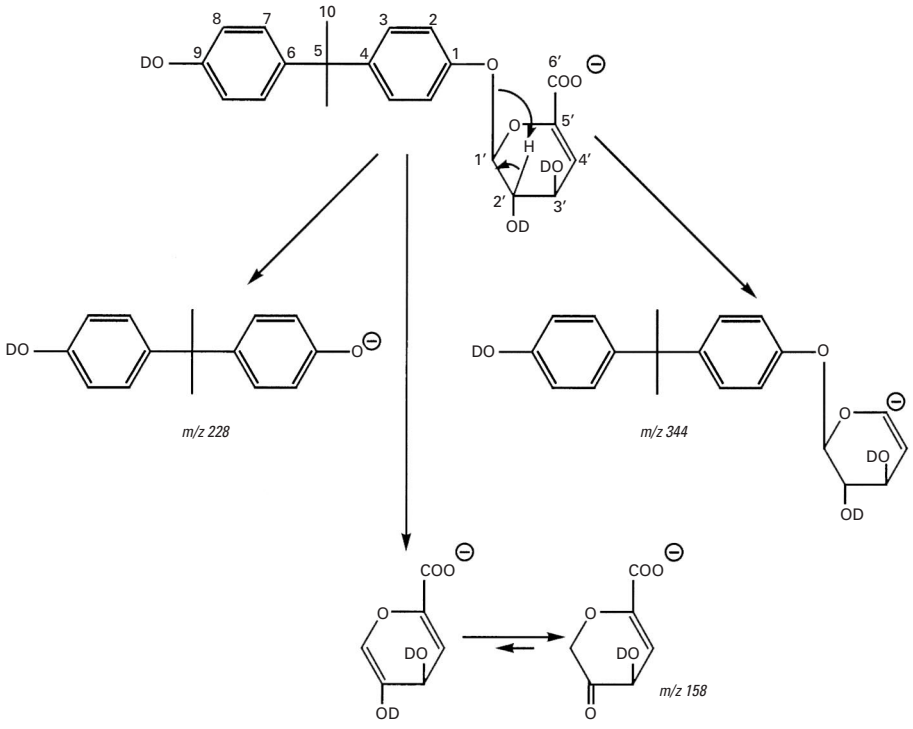

Figure 4. Proposed decomposition pathway of the *m/z* 388 $[Md4–D]^-$ ion of GlcA DH-BPA submitted to MS/MS.

Table 3. Metabolite distribution in bile, digestive tract, and feces of mice dosed subcutaneously with 25 µg/kg ^3H-BPA at day 17 of gestation.

Metabolite	GlcA-BPA-OH	22a/22b	F	GlcA-BPA	GlcA DH-BPA	HO_3S-BPA HO-BPA	BPA	NI
R_t (min)	11.5	22	23.7	25	29	31.5–32.5	33.5	
Bile	3.0 ± 1.5		0.8 ± 0.8	92 ± 3.6	2.3 ± 2.0		1.4 ± 1.2	
Digestive tract	3.0 ± 1.4	2.0 ± 1.5	1.0 ± 0.9	38 ± 12	29.4 ± 14.4	0.2 ± 0.3	23 ± 7.0	2.8 ± 1.9
Feces		0.9 ± 0.2				1.0 ± 1.3	96 ± 1.2	3.3 ± 1.7

Abbreviations: NI, unidentified metabolites; F, R_t corresponding to metabolite F; all other structures are detailed in Table 2. Results are presented as mean percentage ± SD (*n* = 3 animals) on the basis of sample extracts analyses carried out 24 hr after BPA dosage.

MS analysis of the radioactive peak of metabolites 22a, 22b, 22c, and 22d with an R_t of 22 min led to different results, depending on the extracted matrix.

When isolated from the digestive tract, this peak included two different structures. For the first one, the $[M–H]^-$ ion was detected at *m/z* 481. Under resonant excitation conditions, this *m/z* 481 ion decomposed into the *m/z* 401 ion by SO_3 elimination from a sulfate group. The MS^3 spectrum of the *m/z* 401 ion resulting from the decomposition of the *m/z* 481 ion showed a fragment ion at *m/z* 243, corresponding to hydroxylated BPA. No water loss was observed for the *m/z* 401 ion, suggesting that the hydroxylation took place on the aromatic cycle rather than on one of the methyl groups of BPA. In the same way observed for GlcA DH-BPA, the formation of the *m/z* 243 ion from the selected *m/z* 401 parent ion should correspond to the elimination of a neutral dehydrated glucuronide moiety. Therefore, metabolite 22a was tentatively identified as a double conjugate (sulfate/dehydrated glucuronide) of hydroxylated BPA, as indicated in Table 2. The second compound evidenced from the mass spectrum presented a $[M–H]^-$ quasi-molecular ion at *m/z* 495, indicating the presence of an additional methyl group, when compared with 22a. Moreover, its fragmentation pathway was similar to that of 22a, i.e., loss of sulfate (*m/z* 415, MS^2) and loss of a dehydrated glucuronide (*m/z* 257, MS^3). The latter ion dissociation evidenced an additional methyl loss (*m/z* 242, MS^4). Thus, metabolite 22b should correspond to the double conjugate (sulfate/dehydrated glucuronide) of methoxylated BPA.

When isolated from urine, again, two metabolites could be evidenced from the full spectrum of the R_t 22 min peak, but the structures evidenced were not metabolites 22a and 22b. Both 22c and 22d showed a close fragmentation pattern, the respective $[M\text{-}H]^-$ ions being detected at *m/z* 499 (22c) and *m/z* 515 (22d). MS^2 and MS^3 analyses (see Table 2) demonstrated that both were double conjugates (sulfate/Glc). MS^4 and MS^5 fragmentation indicated the successive loss of two methyl groups. Moreover, the MS^6 spectra from both *m/z* 499 and *m/z* 515 showed an *m/z* 109 fragment ion characteristic of a doubly hydroxylated aromatic cycle. For the *m/z* 515 ion, a third methyl group loss was also observed (*m/z* 228). Thus, it is hypothesized that 22c is a Glc/sulfate double conjugate of methoxylated BPA and 22d, the same structure bearing an additional hydroxy group.

HO_3S-BPA, with an R_t of 31.5 min, was identified from both urine and feces. This metabolite gave a $[M–H]^-$ quasi-molecular ion at *m/z* 243. Decomposition of this ion (in MS^2 experiment) led to a fragment ion at *m/z* 227 corresponding to deprotonated BPA, indicating a loss of SO_3 from a sulfate group. This allowed us to consider this metabolite as a sulfate conjugate of BPA.

HO-BPA was identified from fecal extracts. Because it was detected in very low amounts and was not perfectly separated from HO_3S-BPA by HPLC, we choose to quantify both metabolites together (see Table 3). The mass spectrometric analysis of this metabolite showed an ion at *m/z* 243. This *m/z* value was consistent with that of the $[M–H]^-$ deprotonated ion of hydroxylated BPA. This was confirmed by the MS^2 spectrum, showing decomposition into a fragment ion at *m/z* 228 by loss of a methyl group. The presence of low abundant fragments at *m/z* 149 and particularly at *m/z* 109 were diagnostic of aromatic hydroxylation (Table 2). Hence, these results suggest that this metabolite arises from an aromatic hydroxylation of BPA. We cannot rule out the possibility that HO-BPA would also be excreted in urine, although it has not been characterized directly from this matrix.

Table 4. ^{13}C and ^1H chemical shifts of GlcA DH-BPA[a,b] (atom numbering according to Figure 4).

Atom	δ ^{13}C[c]	δ ^1H
1	155.90	—
2	117.06	7.08 (d) J = 8.9 Hz
3	128.12	7.13 (d) J = 8.9 Hz
4	146.13	—
5	42.11	—
6	142.54	—
7	128.07	7.01 (d) J = 8.7 Hz
8	114.93	6.65 (d) J = 8.7 Hz
9	155.39	—
10	30.95	1.59 (s)
1′	100.29	5.46 (d) J = 5.8 Hz
2′	71.72	3.84 (t) J = 5.5 Hz
3′	68.28	4.16 (dd) J = 5.0, 4.0 Hz
4′	108.29	5.90 (d) J = 3.5 Hz
5′	145.83	—
6′[d]	NO[d]	—

[a]In ppm from trimethylsylane; solvent: CD_3OD. [b]Assignments obtained from 2D measurements. [c]Determined from the cross sections of HMBC and HMQC diagrams. [d]Signal not observed.

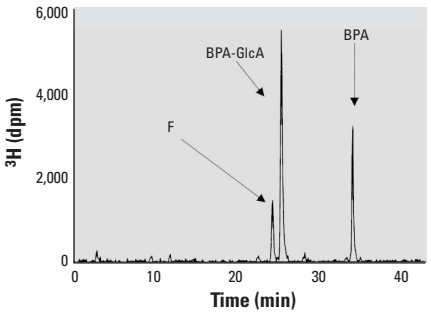

Figure 5. Typical radio-chromatographic profile obtained for fetus extracts after mice subcutaneous dosage with 25 µg/g ^3H-BPA. The displayed chromatogram was obtained 2 hr after BPA dosage (lot II).

BPA Metabolite Study in Maternal Tissues and Fetuses

Metabolic profiles. Radio-chromatographic profiles were obtained individually for all lot I, II, and III mice amniotic fluids, placentas, plasmas, livers, and fetuses (pool of three). They were qualitatively similar for these different biologic matrices, though quantitative differences were observed. Moreover, they were also similar for lot IV mice, which have been used for metabolite isolation. A representative fetal extract analysis is shown in Figure 5. Unchanged BPA, GlcA-BPA, and metabolite F were the major compounds detected in all these tissues. Minor metabolites were also detected, and could correspond, on the basis of their R_t, to structures already identified from urine and digestive tracts extracts: GlcA-BPA-OH and GlcA-BPA-Glc, as well as HO_3S-BPA (and/or HO-BPA), GlcA DH-BPA, and trace amounts of metabolites eluted with an R_t of 22 min (only for liver extracts).

Metabolite quantification. Because we had established that the proportion of nonextractable radioactivity and extractable volatile radioactivity varied for lots I, II, and III (Figure 1), actual concentrations of the major metabolites present in the reproductive tract, liver, and fetuses were calculated in nanograms per gram, on the basis of the amount of nonvolatile extractable radioactivity present in these tissues and analyzed by radio-HPLC. Results are presented in Table 5. The major compound in all samples was GlcA-BPA, except the placenta, where unchanged BPA and metabolite F represented more than 70% (at 0.5 hr) and about 60% (at 24 hr), respectively, of the analyzed radioactivity, according to their HPLC R_ts. BPA concentration decreased quickly, as well as that of most minor metabolites. However, except for plasma, the proportion of metabolite F increased with time, and its concentration rose in placentas and amniotic fluids. In maternal livers, the proportion of the three major metabolites was relatively stable between 0.5 and 24 hr.

Metabolite identification. The structures of BPA and GlcA-BPA were confirmed after the isolation of metabolites from both liver and fetuses. For liver, the radioactive peak with an R_t of 22 min was also isolated, and when submitted to ESI-MS, this sample produced results similar to those established for the same R_t peak obtained from urine, evidencing metabolites 22c and 22d.

The structure of metabolite F, purified from fetus extracts, was studied by ESI/MS in both negative and positive ionization modes (Figure 6). Its MS analysis produced identical results when F was isolated from liver extracts.

The negative ESI analysis of F gave an $[M– H]^-$ ion at *m/z* 606, indicating an odd molecular weight (607) and thus the presence

of an odd number of nitrogen atoms (Figure 6A). MS^2 experiments carried out on this ion evidenced the formation of an *m/z* 385 ion, and thus the loss of 221 mass units. Further fragmentation of the *m/z* 385 ion was similar to that of GlcA DH-BPA.

Under positive ESI conditions, quasi-molecular $[M+H]^+$ and $[M+Na]^+$ species were detected at *m/z* 608 and 630, respectively (Figure 6B). The MS2 spectrum of the $[M+H]^+$ ion exhibited an *m/z* 204 ion, with the loss of 404 mass units corresponding to a glucuronide conjugate of BPA. Thus, F could not be a metabolite in which BPA was conjugated to a dehydrated glucuronide. An *m/z* 380 ion fragment (formed by the loss of BPA) was also observed in MS^2, suggesting that the *m/z* 204 ion arose from a moiety directly linked to the glucuronide. Further dissociation of the *m/z* 204 ion led to *m/z* 186 (loss of a molecule of water, MS^3), which itself gave *m/z* 168 (loss of a molecule of water) and *m/z* 144 (loss of CH_2CO) when submitted to MS^4 analysis, indicating the presence of an acetyl group.

All data from these two complementary analyses were consistent with a structure where BPA glucuronide was linked to an acetylated galactosamine (or glucosamine). Thus it was hypothesized that metabolite F was a GlcA conjugate of BPA, the GlcA itself being conjugated to *N*-acetyl-galactosamine (or *N*-acetyl glucosamine). Though the eventuality that these conjugations would take place on the two phenols of BPA cannot totally be ruled out, our MS data, with the observation of an $[M+H]^+$ *m/z* 380 ion (corresponding to the disaccharide moiety), indicate that *N*-acetyl galactosamine should be linked directly to one of the hydroxyl groups of the GlcA. Because it was impossible to submit metabolite F to NMR analysis because of the low quantities available, we purified this compound from remaining lots I, II, and III fetuses and conduced enzymatic experiments on the compound using either *N*-acetyl glucosaminidase or *N*-acetyl galactosaminidase. In the first case, metabolite F was left unchanged after the incubation, whereas the second enzyme produced a 100% radio-HPLC shift of F (R_t, 24 min) to the R_t of GlcA-BPA (25 min). This R_t shift was confirmed by the radio-HPLC analysis of a known amount of metabolite F for which 50% had been incubated with *N*-acetyl galactosaminidase and 50% was not, demonstrating that F and GlcA-BPA were perfectly separated (Figure 7). Thus, it was concluded metabolite F was a double conjugate of BPA to GlcA and *N*-acetyl galactosamine, for which a possible structure is displayed in Figure 8.

Discussion

The present study was carried out in pregnant CD1 mice at a late stage of gestation with a nominal dosage of 25 µg/kg BPA, corresponding to an actual dosage of 20–23 µg/kg. The goal was to investigate the metabolic fate of BPA in an animal model in which this chemical alters the genital tract and mammary gland when administered at low doses during gestation (*13,14,18,19,22,23,45*). The core study focused on the development of analytic methods allowing us to characterize the structure of BPA metabolites both in maternal tissues and fetuses, 0.5, 2, and 24 hr after BPA was injected by subcutaneous route. Additional information was acquired from pregnant mice dosed subcutaneously with 50 mg/kg BPA and nonpregnant mice dosed orally with 25 µg/kg BPA, allowing some comparisons with previously reported pharmacokinetic data (*9,35,42,43*).

Metabolic balance studies showed that BPA residues were mainly excreted through the digestive tract, in accordance with previous works carried out in rats (*3,34,35*). At 24 hr, 21% and 6% of the radioactivity injected to pregnant mice had been excreted in feces and urine, respectively; the digestive tract and its content accounting for an additional 45%. The total amount of radioactivity recovered from gall bladders represented less than 2% of the dosage. Because animals were not fed during the 24-hr experiment, we assume that significant gall bladder content emptying into the duodenum did not occur. It is possible that a large part of the BPA residues recovered in feces and digestive tracts had actually been directly secreted by the intestine. Such a mechanism has already been demonstrated for other xenobiotics (*47,48*). It cannot be ruled out that the enterohepatic cycling kinetics of BPA may have been modified by the fact that the animals had not been fed during the experiment. However, previous statements that BPA residues undergo extensive biliary excretion (*9,43,49*) deserve more investigation, particularly in mice.

Measured blood radioactivity levels averaged 2–4 ng/g of BPA equivalent in pregnant mice, which is related to the use of a very low dose of BPA. No direct comparison of these results can be established with pharmacokinetic data obtained from rodents dosed in the high microgram per kilogram range (*42*) or the milligram per kilogram range (*9,35,42,43*). Results 0.5 hr after BPA injection showed that

Table 5. Qualitative analysis of the radioactivity extracted from maternal plasma, liver, placenta, amniotic fluid, and fetuses for lot I, II, and III mice dosed subcutaneously with 25 µg/kg ^{3}H-BPA.

	GlcA-BPA-OH		GlcA-BPA-Glc		Metabolite F		GlcA-BPA		BPA		Others[a]
R_t	11.5 ng/g	%	17.5 ng/g	%	24.0 ng/g	%	25.0 ng/g	%	33.5 ng/g	%	%
Maternal plasma											
0.5 hr	0.07 ± 0.01	3	0.11 ± 0.02	4	0.11 ± 0.02	4	1.01 ± 0.19	39	1.06 ± 0.19	41	9
2 hr	0.02 ± 0.01	2	0.03 ± 0.01	4	0.03 ± 0.01	4	0.55 ± 0.14	63	0.15 ± 0.04	17	10
24 hr	0.04 ± 0.04	20		0		0	0.13 ± 0.05	65		0	15
Placenta											
0.5 hr		0		0	0.46 ± 0.48	2	5.50 ± 4.24	25	15.98 ± 12.02	72	1
2 hr	0.03 ± 0.02	1	0.04 ± 0.03	1	0.37 ± 0.07	7	3.13 ± 2.34	62	1.32 ± 0.95	26	3
24 hr	0.05 ± 0.04	5	0.04 ± 0.02	4	0.64 ± 0.19	59	0.21 ± 0.22	19	0.06 ± 0.04	6	6
Fetus											
0.5 hr	0.05 ± 0.03	1	0.04 ± 0.04	0	0.46 ± 0.27	5	3.83 ± 2.65	44	4.20 ± 2.16	49	1
2 hr	0.02 ± 0.02	1	0.01 ± 0.02	0	0.37 ± 0.22	13	1.93 ± 0.45	66	0.48 ± 0.55	16	3
24 hr	0.01 ± 0.01	1		0	0.11 ± 0.07	13	0.51 ± 0.12	60	0.13 ± 0.16	15	2
Amniotic fluid											
0.5 hr	0.10 ± 0.14	1	0.19 ± 0.14	2	0.09 ± 0.13	1	8.17 ± 6.55	83	0.90 ± 0.89	9	4
2 hr	0.06 ± 0.03	1	0.07 ± 0.03	1	0.26 ± 0.15	5	4.82 ± 4.81	88	0.10 ± 0.07	2	2
24 hr	0.13 ± 0.05	8	0.01 ± 0.02	1	0.37 ± 0.09	24	0.70 ± 0.13	44	0.03 ± 0.03	2	20
Maternal liver											
0.5 hr	0.12 ± 0.12	0	0.18 ± 0.24	0	6.22 ± 1.75	18	12.90 ± 2.81	37	10.85 ± 2.77	31	12
2 hr	0.08 ± 0.08	1	0.77 ± 0.25	8	2.16 ± 0.91	20	4.95 ± 1.82	45	1.51 ± 0.97	13	13
24 hr	0.16 ± 0.14	2	0.35 ± 0.13	7	0.99 ± 0.42	16	2.56 ± 1.62	36	1.72 ± 1.18	23	17

Results are expressed in nanograms per gram and as a percentage of the extracted radioactivity for the major compounds detected.
[a]Sum of all unlisted metabolites.

when administered through a parenteral route, BPA was readily absorbed and distributed and was found in ovaries, uterus, and fetuses. Radioactivity levels decreased quickly, and the amount of BPA residues detected at 2 and 24 hr were not significantly different. At 24 hr, the highest concentration of residue was measured in the liver (12 ng/g), whereas less than 1 ng/g was detected in fat. The main difference between samples collected at 2 and 24 hr was qualitative; the latter ones contained a greater proportion of volatile radioactivity that could be a result of tritium exchange and/or related to the metabolic breakdown of BPA into very small molecules. For both time points, the amount of extractable residues was higher in livers, placentas, fetuses, and amniotic fluids than in the corresponding plasmas.

Fecal radioactivity was mainly associated with unchanged BPA, although traces of HO_3S-BPA and HO-BPA were detected. Bile residues mainly consisted of GlcA-BPA. Intestinal bacteria are often responsible for the deconjugation of biliary glucuronides into the parental xenobiotic (*50*), and indeed most of the fecal radioactivity was detected as unchanged BPA. However, digestive tract extractions and subsequent radio-chromatographic analyses not only demonstrated the presence of BPA and GlcA-BPA, but also that of another major metabolite whose structure was that of a dehydrated glucuronide conjugate of BPA (GlcA DH-BPA). To our knowledge, the dehydration of a glucuronide conjugate by mammalian biotransformation systems or bacterial enzymes has never been documented. However, both NMR and MS experiments, including tritium/deuterium exchange experiments unequivocally supported this structural characterization. In terms of biologic activity, it is now well established that GlcA-BPA is a far less potent estrogen than BPA itself (*39,41*). The estrogenic potency of the corresponding dehydrated conjugate (GlcA DH-BPA) is unknown, but this major intestinal metabolite was only detected in trace amounts in all other tissues examined during this study.

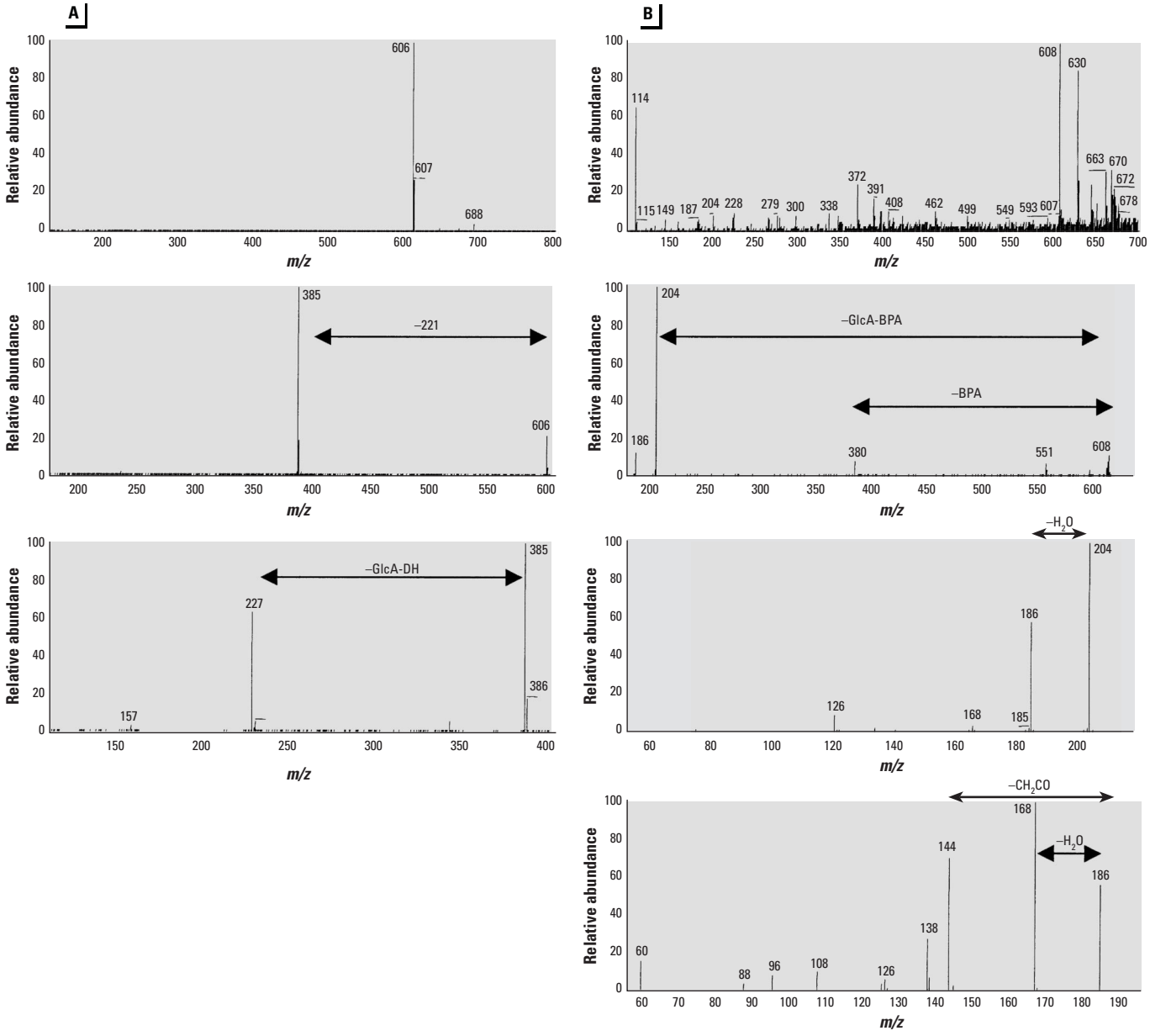

Figure 6. ESI-MS^n analyses for metabolite F isolated from fetus extracts: mass spectra recorded in negative (*A*) and positive (*B*) ionization modes. A: MS, MS^2 606, and MS^3 385; B: MS, MS^2 608, MS^3 204, and MS^4 186 spectra.

The two major urinary metabolites detected by radio-HPLC were GlcA-BPA, as already evidenced in rat (*3,34,35*), and a newly identified GlcA conjugate of hydroxylated BPA, in which the hydroxylation takes place on one of the methyl groups of BPA (GlcA-BPA-OH). Its corresponding aglycone was not detected. However, this metabolite is of potential interest because its structure would not exclude estrogenic activity. Only a low amount of unchanged BPA was detected, whatever the BPA dosage or administration route. Several double-conjugated metabolites of BPA were characterized from urine. Two of them (metabolites 22c and 22d), also identified from liver extracts, were conjugates of methoxylated BPA, which supports the results of previous *in vitro* studies in rats (*38*) and humans (*39*) indicating an aromatic hydroxylation of BPA into catechol-BPA (3-hydroxy-BPA). The present results demonstrate that this metabolic pathway does exist *in vivo*. Catechol-BPA is a reactive compound able to bind to DNA *in vitro* (*33*), possibly following the formation of BPA-*o*-quinone. In CD1 mice, this compound was excreted in urine after being methylated (very likely by catechol-*O*-methyl-transferase) and conjugated. The existence of this metabolic route was also supported by the identification in digestive tract extracts of two structurally close metabolites (22a and 22b). *In vivo* biotransformation of BPA into 3-hydroxy-BPA may explain the formation of part of the unextractable residues detected in tissues, but is not expected to enhance the biologic activity of BPA, as this metabolite is supposed to be a less potent estrogen than BPA (*38,39*).

The use of [^{3}H]-BPA enabled a precise monitoring of the residues present in livers, plasma, and reproductive tracts of mothers, as well as in fetuses. Radio-chromatograms obtained for all these tissues were qualitatively similar. Calculations based on the respective proportions of extractable radioactivity and direct MS structural characterization from fetus extracts led to the quantification of the three major metabolites, namely GlcA-BPA, metabolite F, and unchanged BPA. It should be stressed that regardless of the matrix assayed, we found no qualitative difference between mice dosed by subcutaneous or oral route. BPA bioavailability was indeed lower when administered orally, but in our opinion the differences previously observed in rat for the respective plasmatic radio-chromatograms (*35*) depend not on the route of administration but on the sensitivity of the applied methods.

The passage of BPA through the placental barrier was demonstrated, corroborating previous results obtained in rats fed with a high oral dosage of BPA (*9,44*). In CD1 mice, the transportation of BPA into fetuses occurred rapidly, as shown by its hepatic, plasmatic and fetal concentrations at 0.5 hr (about 10, 1, and 4 ng/g, respectively). At this time point, calculated GlcA-BPA concentrations in the fetus were similar to that of unchanged BPA. A recent publication suggested that GlcA-BPA could not cross the placental barrier in a rat model (*36*). Although our data do not rule out the possibility that GlcA-BPA may cross the placental barrier in CD1 mice, it is likely that its presence in fetal tissue is due to fetal glucuronidation, as the GlcA-BPA concentration in amniotic fluids was always far above that of unchanged BPA. In near-term rodents, both fetal glucuronidation and hydroxylations have previously been strongly hypothesized for DES, a potent synthetic estrogenic compound (*51*). Hydroxylated BPA metabolites were not identified in fetus extracts of CD1 mice, but their formation cannot be ruled out, because the production of catechol-BPA may partly explain that of bound residues (at 24 hr, 0.25 ng/g of the fetal radioactivity was not extractable). Though BPA is a far less potent estrogen than DES, the two compounds, which share some structural characteristics, also share metabolic similarities in rodents. Moreover, in pregnant female rats administered a parenteral dosage of DES, fetal residual levels were 2–3 times greater than those measured in the mother's blood (*51*); there results are comparable to those found in the present study for CD1 mice dosed with BPA.

Metabolite F was identified as a disaccharide conjugate of BPA. Though only detected in trace amounts in plasma 24 hr after BPA injection, it accounted for a large proportion of the radioactivity detected in fetuses (10%), maternal livers (20%), amniotic fluid (20%), and placentas (60%). The metabolic pathway leading to the formation of metabolite F and the tissue(s) where it is synthesized remains unknown. Metabolite F may result from the conjugation of GlcA-BPA with *N*-acetyl-galactosamine. However, the conjugation of the sugar moiety of a conjugated xenobiotic by a second sugar is a common metabolic process only in plants. Very few examples of conjugation to an acetylated sugar have been reported. Interestingly, one of the compounds for which a conjugation to *N*-acetyl-glucosamine (an isomer of *N*-acetyl-galactosamine) has been demonstrated is estrone (isolated from pregnant women's bile) (*52*); the double conjugation of the molecule occurs at two different locations of the molecule. Thus, similarities also exist between the metabolic pathways of BPA and that of natural estrogens. It is worth noting that GlcA/*N*-acetyl-galactosamine is the repeating disaccharide found in the glycosaminoglycan moiety (chondroitin sulfate, dermatan sulfate) of proteoglycans, which are major constituents of the extracellular matrix. The biologic significance of the formation of metabolite F and its possible connection with the synthesis of proteoglycans requires further investigation.

We performed this study to understand more precisely the mechanism underlying the low-dose effects of BPA. Understanding the

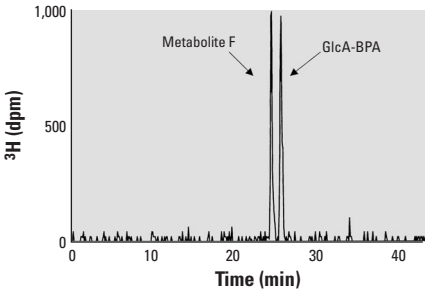

Figure 7. Radio-chromatographic analysis of approximately 3,000 disintegrations per minute (dpm) (50 Bq) of metabolite F incubated with *N*-acetyl galactosaminidase, fortified with an identical amount of metabolite F that was not submitted to enzymatic deconjugation.

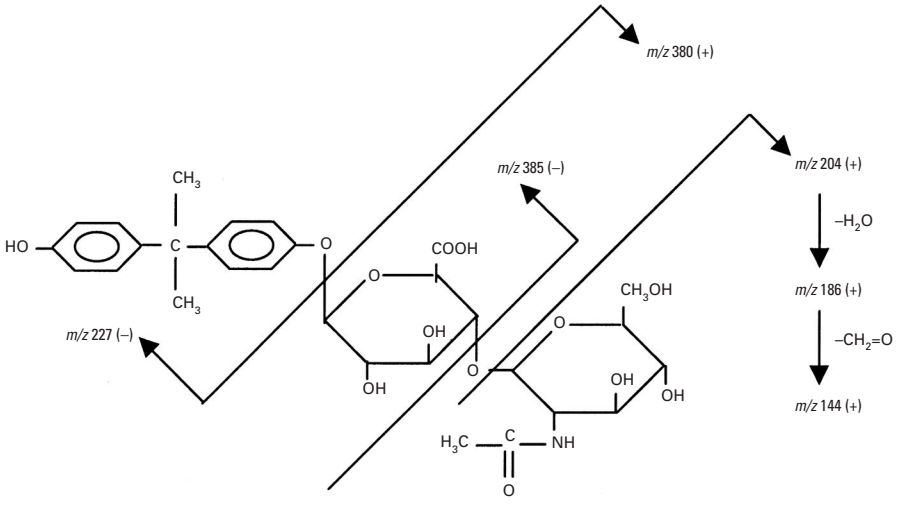

Figure 8. Proposed chemical structure and fragmentation pathways for metabolite F under both positive (+) and negative (–) ESI.

fate of BPA in mammalian animal models is necessary to achieve a sound risk assessment for this compound. Excreta and tissue analyses, including fetuses, have clearly shown that the metabolic pathways of BPA are more complex than previously thought. GlcA-BPA is indeed a major metabolite of BPA, but several other metabolites have been characterized in the present study, among which are several uncommon structures such as Glc conjugates, dehydrated glucuronides, and a disaccharide, which represent a large part of the fetal and hepatic radioactivity. None of these metabolites is expected to possess an enhanced estrogenic potency, suggesting that the estrogenic effect of BPA derives from the parental compound. However, these BPA metabolites have yet to be tested for estrogen activity. A recent study reported that BPA was transformed into a potent estrogenic metabolite by Wistar rat liver S9 fractions; however, its chemical structure was not revealed (*53*). On the basis of the chromatographic behavior of this compound, we conclude it is not detected in CD1 mice *in vivo*. It is unknown whether the absence of this metabolite is caused by lack of synthesis or efficient transformation into more polar compounds.

The results reported here support the hypothesis that the endocrine disruptor activity of BPA, if due exclusively to its estrogenic activity, could be mainly attributed to the parent compound. BPA easily crosses the placental barrier and is present both in fetuses and in the reproductive tract of mothers. In addition, the *in vivo* characterization of several metabolites suggests that this xenoestrogen could be metabolized into reactive intermediates. The metabolic fate of BPA should be thoroughly studied in mammals, including humans, to understand the biologic consequences of exposure.

References and Notes

1. Brotons JA, Olea-Serrano MF, Villalobos M, Pedraza V, Olea N. Xenoestrogens released from lacquer coatings in food cans. Environ Health Perspect 103:608–612 (1995).
2. The Bisphenol A Homepage. Industry Responds to WWF Report on Bisphenol A. Available: http://bisphenol-a.org/new/052800.html [cited 7 February 2002].
3. Knaak JB, Sullivan LJ. Metabolism of bisphenol A in the rat. Toxicol Appl Pharmacol 8:175–184 (1966).
4. Feldman D, Krishnan A. Estrogens in unexpected places: possible implications for researchers and consumers. Environ Health Perspect 103(suppl 7):129–133 (1995).
5. Olea J, Pulgar R, Perez P, Olea-Serrano F, Rivas A, Novillo-Fertrell A, Pedraza V, Soto AM, Sonnenschein C. Estrogenicity of resin-based composites and sealants used in dentistry. Environ Health Perspect 104:298–305 (1995).
6. Yamamoto T, Yasuhara A, Shiraishi H, Nakasugi O. Bisphenol A in hazardous waste landfill leachates. Chemosphere 42:415–418 (2001).
7. Staples CA, Dorn PB, Klecka GM, O'Block ST, Harris LR. A review of the environmental fate, effects, and exposure of bisphenol A. Chemosphere 36:2149–2173 (1998).
8. West RJ, Goodwin PA, Klecka GM. Assessment of the ready biodegradability of bisphenol A. Bull Environ Contam Toxicol 67:106–112 (2001).
9. Takahashi O, Oishi S. Disposition of orally administered 2,2-bis(4-hydroxyphenyl)propane (bisphenol A) in pregnant rats and the placental transfer to fetuses. Environ Health Perspect 108:931–935 (2000).
10. Soto AM, Sonnenschein C. The role of estrogens on the proliferation of human breast tumor cells (MCF7). J Steroid Biochem 23:87–94 (1985).
11. Fang H, Tong W, Shi LM, Blair R, Perkins R, Branham W, Hass BS, Xie Q, Dial SL, Moland CL, et al. Structure-activity relationships for a large diverse set of natural, synthetic, and environmental estrogens. Chem Res Toxicol 14:280–294 (2001).
12. Hiroi H, Tsutsumi O, Momoeda M, Takai Y, Osuga Y, Taketani Y. Differential interactions of bisphenol A and 17β-estradiol with estrogen receptor α (ERα) and ERβ. Endocr J 46:773–778 (1999).
13. Nagel SC, vom Saal FS, Thayer KA, Dhar MG, Boechler M, Welshons WV. Relative binding affinity-serum modified access (RBA-SMA) assay predicts the relative *in vivo* bioactivity of the xenoestrogens bisphenol A and octylphenol. Environ Health Perspect 105:70–76 (1997).
14. Welshons WV, Nagel SC, Thayer KA, Judy BM, vom Saal FS. Low-dose bioactivity of xenoestrogens in animals: fetal exposure to low doses of methoxychlor and other xenoestrogens increases adult prostate size in mice. Toxicol Ind Health 15:12–25 (1999).
15. Ashby J, Tinwell H, Haseman J. Lack of effects for low dose levels of bisphenol A and diethylstilbestrol on the prostate gland of CF1 mice exposed *in utero*. Regul Toxicol Pharmacol 30:156–166 (1999).
16. Cagen SZ, Waechter JM, Dimond S, Breslin WJ, Butala JH, Jekat FW, Joinner RL, Shiotsuka GE, Harris LR. Normal reproductive organ development in CF-1 mice following prenatal exposure to bisphenol A. Toxicol Sci 50:36–44 (1999).
17. Kaiser J. Panel cautiously confirms low-dose effects. Science 290:695–696 (2000).
18. vom Saal FS, Cooke PS, Buchanan DL, Palanza P, Thayer KA, Nagel SC, Parmigiani S, Welshons WV. A physiologically based approach to the study of bisphenol A and other estrogenic chemicals on the size of reproductive organs, daily sperm production, and behavior. Toxicol Ind Health 14:239–260 (1998).
19. Gupta C. Reproductive malformation of the male offspring following maternal exposure to estrogenic chemicals. Proc Soc Exp Biol Med 224:61–68 (2000).
20. Gupta C. The role of estrogen receptor, androgen receptor and growth factors in diethylstilbestrol-induced programming of prostate differentiation. Urol Res 28:223–229 (2000).
21. Ramos JG, Varayoud J, Sonnenschein C, Soto AM, Munoz De Toro M, Luque EH. Prenatal exposure to low doses of bisphenol A alters the periductal stroma and glandular cell function in the rat ventral prostate. Biol Reprod 65:1271–1277 (2001).
22. Howdeshell KL, Hotchkiss AK, Thayer KA, Vandembergh JG, vom Saal FS. Exposure to bisphenol A advances puberty. Nature 401:401–402 (1999).
23. Markey CM, Luque EH, Munoz de Toro M, Sonnenschein C, Soto AM. *In utero* exposure to bisphenol A alters the development and tissue organization of the mouse mammary gland. Biol Reprod 65:1215–1223 (2001).
24. Rubin BS, Murray MK, Damassa DA, King JC, Soto AM. Perinatal exposure to low doses of bisphenol A affects body weight, patterns of estrous cyclicity, and plasma LH levels. Environ Health Perspect 109:675–680 (2001).
25. Markey CM, Michaelson CL, Veson EC, Sonnenschein C, Soto AM. The mouse uterotrophic assay: a reevaluation of its validity in assessing the estrogenicity of bisphenol A. Environ Health Perspect 109:55–60 (2001).
26. Soto AM, Chung KL, Sonnenschein C. The pesticides endosulfan, toxaphene, and dieldrin have estrogenic effects on human estrogen-sensitive cells. Environ Health Perspect 102:380–383 (1994).
27. Soto AM, Fernandez MF, Luizzi MF, Oles Karasko AS, Sonnenschein C. Developing a marker of exposure to xenoestrogen mixtures in human serum. Environ Health Perspect 105(suppl 3):647–654 (1997).
28. Rajapakse N, Ong D, Kortenkamp A. Defining the impact of weakly estrogenic chemicals on the action of steroidal estrogens. Toxicol Sci 60:296–304 (2001).
29. Farabollini F, Porrini S, Dessi-Fulgherit F. Perinatal exposure to the estrogenic pollutant bisphenol A affects behavior in male and female rats. Pharmacol Biochem Behav 64:687–694 (1999).
30. Kubo K, Arai O, Ogata R, Omura M, Hori T, Aou S. Exposure to bisphenol during the fetal and suckling periods disrupts sexual differentiation of the locus coeruleus and the behavior in the rat. Neurosci Lett 304:73–76 (2001).
31. Takahashi S, Chi XJ, Yamaguchi Y, Suzuki H, Sugaya S, Kita K, Hiroshima K, Yamamori H, Ichinose M, Suzuki N. Mutagenicity of bisphenol A and its suppression by interferon-alpha in human RSa cells. Mutat Res 490:199–207 (2001).
32. Tsutsui T, Tamura Y, Suzuki A, Hirose Y, Kobayashi M, Nishimura H, Metzler M, Barrett JC. Mammalian cell transformation and aneuploidy induced by five bisphenols. Int J Cancer 86:154–154 (2000).
33. Atkinson A, Deodutta R. *In vitro* conversion of environmental estrogenic chemical bisphenol A to DNA binding metabolite(s). Biochem Biophys Res Commun 210:424–433 (1995).
34. Snyder RW, Maness SC, Gaido KW, Welsch F, Sumner SCJ, Fennell TR. Metabolism and disposition of bisphenol A in female rats. Toxicol Appl Pharmacol 168:225–234 (2000).
35. Pottenger LH, Domoradzky JY, Markham DA, Hansen SC, Cagen SZ, Waechter JM. The relative bioavailability and metabolism of bisphenol A in rats is dependent upon the route of administration. Toxicol Sci 54:3–18 (2000).
36. Miyakoda H, Tabata M, Onodera S, Takeda K. Comparison of conjugative activity, conversion of bisphenol A to bisphenol A glucuronide in fetal and mature rat. J Health Sci 46:269–274 (2000).
37. Nakagawa Y, Tayama S. Metabolism and cytotoxicity of bisphenol A and other bisphenols in isolated rat hepatocytes. Arch Toxicol 74:99–105 (2000).
38. Nakagawa Y, Suzuki T. Metabolism of bisphenol A in isolated rat hepatocytes and estrogenic activity of a hydroxylated metabolite in MCF-7 human breast cancer cells. Xenobiotica 31:113–123 (2001).
39. Elsby R, Maggs JL, Ashby J, Park BK. Comparison of the modulatory effects of human and rat liver microsomal metabolism on the estrogenicity of bisphenol A: implications for extrapolation to humans. J Pharmacol Exp Ther 297:103–113 (2001).
40. Yokota H, Iwano H, Endo M, Kobayashi T, Inoue H, Ikushiro SI, Yuasa A. Glucuronidation of the environmental oestrogen bisphenol A by an isoform of UDP-glucuronosyltransferase, UGT2B1, in the rat liver. Biochem J 340:405–409 (1999).
41. Matthews JB, Twomey K, Zacharewski TR. *In vitro* and *in vivo* interactions of bisphenol A and its metabolite, bisphenol A glucuronide, with estrogen receptors α and β. Chem Res Toxicol 14(2):149–157 (2001).
42. Yoo SD, Shin BS, Kwack SJ, Lee BM, Park KL, Han SY, Kim HS. Pharmacokinetic disposition and tissue distribution of bisphenol A in rats after intravenous administration. J Toxicol Environ Health A 60:131–139 (2000).
43. Upmeier A, Degen GH, Diel P, Michna H, Bolt HM. Toxicokinetics of bisphenol A in female DA/Han rats after a single i.v. and oral administration. Arch Toxicol 74:431–436 (2000).
44. Miyakoda H, Tabata M, Onodera S, Takeda K. Passage of bisphenol A into the fetus of the pregnant rat. J Health Sci 45:318–323 (1999).
45. Padilla-Banks E, Jefferson WN, Newbold RR. The immature mouse is a suitable model for detection of estrogenicity in the uterotropic bioassay. Environ Health Perspect 109:821–826 (2001).
46. Timms BG, vom Saal FS. Low dose effects of endocrine disrupting chemicals. Presented at the Endocrine Disruptors: Low Dose Peer Review Meeting, NIEHS, NIH, October 2000, Raleigh, NC.
47. Arimori K, Nakano M. Drug exsorption from blood into the gastrointestinal tract. Pharm Res 15: 371–376 (1998).
48. Struble CB. *In situ* intestinal absorption of 2-chloro-*N*-isopropylacetanilide (propachlor) and non-biliary excretion of metabolites into the intestinal tract of rats, pigs and chickens. Xenobiotica 21:85–95 (1991).
49. Inoue H, Yokota H, Makino T, Yuasa A, Kato S. Bisphenol A glucuronide, a major metabolite in rat bile after liver perfusion. Drug Metab Dispos 29:1084–1087 (2001).
50. Scheline RR. Metabolism of foreign compounds by gastrointestinal microorganisms. Pharmacol Rev 25:451–523 (1973).
51. Miller RK, Heckmann ME, McKenzie RC. Diethylstilbestrol: placental transfer, metabolism, covalent binding and fetal distribution in the Wistar rat. J Pharmacol Exp Ther 220:358–365 (1982).
52. Miyazaki T, Kirdani RY, Slaunwhite WR, Sandberg AA. Studies on phenolic steroids in human subjects. XV. Biliary and urinary excretion patterns of estrone. J Clin Endocr 33:128–137 (1971).
53. Yoshihara S, Makishima M, Suzuki N, Ohta S. Metabolic activation of bisphenol A by rat liver S9 fraction. Toxicol Sci 62:221–227 (2001).